

## Type-I–type-II transition in ultra-short-period GaAs/AlAs superlattices

R. Cingolani,\* L. Baldassarre, M. Ferrara, and M. Lugarà

*Dipartimento di Fisica, Università degli Studi di Bari, via Amendola 173, I-70125 Bari, Italy*

K. Ploog

*Max-Planck-Institut für Festkörperforschung, Heisenbergstrasse 1,  
Postfach 80 06 65, D-7000 Stuttgart 80, Federal Republic of Germany*

(Received 29 November 1988; revised manuscript received 14 February 1989)

We report the direct observation of the transition from type I to type II in  $(\text{GaAs})_m/(\text{AlAs})_n$  ultra-short-period superlattices with  $m=n$  by means of photoacoustic spectroscopy and high-excitation-intensity photoluminescence. The transition is found to occur when the constituent superlattice layers have a critical thickness of about 12 monolayers ( $m=n=12$ ). Different temperature dependences of the type-I and type-II recombinations are observed, which are tentatively ascribed to the thermal transfer of the carriers between quantized subbands, in different critical points of the superlattice.

### I. INTRODUCTION

Ultra-short-period  $(\text{GaAs})_m/(\text{AlAs})_n$  superlattices (USPSL) consisting of  $m$  monolayers of GaAs sandwiched between  $n$  monolayers of AlAs have recently attracted considerable interest owing to the staggered alignment of the energy bands of the constituent heterojunctions.<sup>1</sup> In particular, in GaAs/AlAs USPSL with wells and barriers composed of only a few monolayers, the  $\Gamma$  point in the GaAs region lies at energies higher than the  $X$  point in the AlAs region; this results in a potential barrier (from the GaAs  $X$  point) which confines electrons in the  $X$  point of the AlAs layer. As a consequence, these GaAs/AlAs USPSL behave like type-II superlattices, where the lowest energy level has the symmetry properties of the  $X$  point of the AlAs barrier.

Few experimental investigations on the direct-indirect transition induced by an appropriate choice of the layer thicknesses in these superlattices have been carried out.<sup>1–5</sup> Most of the reported data have been obtained by comparing the low-temperature photoluminescence excitation (PLE) spectra with the low-intensity cw photoluminescence spectra showing, with a satisfactory overall agreement, a type-II behavior occurring in  $(\text{GaAs})_m/(\text{AlAs})_n$  superlattices with  $m=n < 15$ .

The aim of this paper is to study in detail the transition from a type-I to type-II superlattice occurring in GaAs/AlAs USPSL at certain critical layer thicknesses. We have combined different spectroscopic techniques in order to obtain an unambiguous interpretation of the observed spectral features. Photoacoustic saturation (PAS) spectroscopy has been used for the first time to study the band-structure properties as a function of  $m$  and  $n$ , for different critical points of the investigated superlattices. The results of PAS have been correlated with the luminescence spectra obtained under intense pulsed excitation from the same USPSL. Conventional low-intensity cw photoluminescence has also been measured and com-

pared with the high-intensity luminescence spectra in order to study the effects of the band filling on the simultaneous optical pumping of the direct and the indirect gap of the USPSL. Finally, the experimental data have been compared with theoretical calculations for the quantized subbands in the superlattices employing a Kronig-Penney formalism based on the Bastard envelope-function approximation.<sup>6</sup>

### II. EXPERIMENTAL

We have investigated several high-quality  $(\text{GaAs})_m/(\text{AlAs})_n$  superlattices with  $2 < n = m < 15$  grown by molecular-beam epitaxy (MBE). The superlattice configurations and characteristics are given in Table I. Details on the growth procedure have been reported elsewhere.<sup>4</sup> Information on the band structure of the investigated USPSL has been obtained by means of photoacoustic (PA) spectroscopy measurements at 300 K. The photoacoustic effect is based on the heat transfer induced by the absorption of photons in a crystal. The PA signal is then given by<sup>7</sup>

$$S(\lambda) = I(\lambda)\beta(\lambda)\alpha(\lambda)[1 - R(\lambda)]F(\lambda)G, \quad (1)$$

where  $I(\lambda)$  is the light-source intensity,  $\beta(\lambda)$  is the absorption coefficient,  $\alpha(\lambda)$  is the fraction of the absorbed light which is converted into heat,  $R(\lambda)$  is the reflectivity of the sample,  $F(\lambda)$  is a function depending on the absorption coefficient of the crystal and on other physical parameters like the thermal diffusivity and the thermal conductance, and  $G$  depends on the experimental arrangement only. When the frequency of the absorbed light is above one of the fundamental absorption edges, the  $F(\lambda)G$  product becomes simply proportional to  $1/\beta$ . Therefore, in Eq. (1) the resulting PA signal becomes independent of the absorption coefficient, i.e., photoacoustic saturation spectroscopy is performed. The PAS spectrum is then given by

TABLE I. Configuration and characteristics of the investigated  $(\text{GaAs})_m/(\text{AlAs})_n$  USPSL.

Sample	(Ref. number)	$m = n$	Period (nm)	Number of periods
1	(41178)	2	1.12	500
2	(41175)	4	2.2	250
3	(5806)	4	2.4	500
4	(41177)	6	3.4	400
5	(5807)	6	3.2	150
6	(5867)	7	4.0	100
7	(41248)	10	5.6	87
8	(41296)	11	6.4	30
9	(41254)	12	6.8	75
10	(41267)	15	8.4	30

$$S(\lambda)/I(\lambda) \sim [1 - R(\lambda)] \quad (2)$$

Hence, in the case of normally incident light the only absorption-coefficient dependence of the PAS signal is contained in the reflectance factor  $R(\lambda)$ . Therefore, light whose frequency is in resonance with some interband transition will lead to a dip in the  $[1 - R(\lambda)]$  spectrum or to a maximum in the  $R(\lambda)$  spectrum (i.e., the normalized PAS spectrum). The PAS signal amplitude was measured in the energy range 2.4–1.6 eV of interest for the  $(\text{GaAs})_m/(\text{AlAs})_n$  USPSL with  $m, n < 15$ . The photoacoustic spectrometer consists of a 300 W high-pressure short-arc Xe lamp whose light is mechanically chopped and dispersed by a dual grating monochromator. The sample cell contains a sensitive microphone transducer with its preamplifier. The light, monitored by a pyroelectric detector to provide the reference signal, impinges normally on the sample in the cell. The reference signal and the PA signal are amplified by two different lock-in amplifiers with a common phase reference signal given by the chopper. Finally, the PA and the pyrometer signals are fed into a ratiometer which provides the output to an X-Y recorder synchronized to the monochromator drive unit.

Luminescence measurements under high-excitation intensity (HEI) have been performed by using a pulsed dye laser, pumped by a  $\text{N}_2$  laser, operating in the spectral range 470–580 nm. The pulse duration was about 5 ns and the power density after focusing has been limited to  $I_0 = 300 \text{ kW cm}^{-2}$ . The luminescence signal has been measured with a box-car detection system and a 0.6 m monochromator equipped with an S-20 photomultiplier tube.

Continuous-wave low-excitation intensity (LEI) luminescence measurements have been performed with a standard lock-in technique by using a cw argon laser. All the luminescence measurements have been performed between 10 and 300 K by using a temperature-controlled closed-cycle He refrigerator.

### III. RESULTS AND DISCUSSION

#### A. Photoacoustic measurements and calculations

In Fig. 1 the normalized PAS spectra obtained from several  $(\text{GaAs})_m/(\text{AlAs})_n$  USPSL at 300 K are shown.

Distinct structures whose energy position varies with the number of monolayers in the USPSL can be detected. In the  $m = n = 2$  USPSL we observe two broad maxima labeled  $\Gamma$  and  $X$  and located around 2.3 and 2.0 eV, respectively. When increasing the number of monolayers the two PAS maxima decrease in energy, approaching each other, and they become nearly coincident in the  $n = m = 12$  USPSL around 1.75 eV. For a larger number of monolayers per period the two structures anticross and the maximum labeled  $X$  lies at higher energy [around 1.7 eV in the  $(\text{GaAs})_{15}/(\text{AlAs})_{15}$  superlattice]. The observed  $m$  dependence of the PAS signal is closely related to the anticrossing of the AlAs  $X$  point and of the GaAs  $\Gamma$  point, occurring when the well width becomes large. It is therefore expected that the energy positions of the maxi-

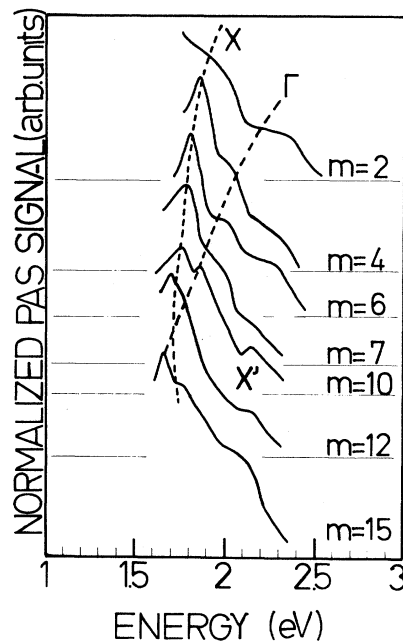


FIG. 1. Normalized photoacoustic saturation spectra of several  $(\text{GaAs})_m/(\text{AlAs})_n$  USPSL superlattices with  $m = n$  and  $m, n$  ranging between 2 and 15. The dashed lines indicating the PAS maxima are drawn as a guide for the eyes.

ma in the PAS spectra should agree with the calculated subband energy positions of the electrons confined at the  $\Gamma$  point of the GaAs layer and at the  $X$  point of the AlAs barrier. In Fig. 2 we show the comparison between the energy position of the observed PAS maxima and the calculated energy positions of the  $\Gamma$  and  $X$  quantized states versus the number of monolayers composing the well and the barrier ( $m=n$ ). The calculations have been performed by using a modified Kronig-Penney formalism in the envelope-function approximation<sup>6</sup> and neglecting the  $\Gamma$ - $X$  mixing effect. The agreement between theory and experiment is satisfactory and is within the experimental uncertainty of the PAS technique (around 30 meV).

In the spectra of Fig. 1 another structure labeled  $X'$  is present. Since it is related to the PA resonance in the  $X$  point of the bulk AlAs layer (around 2.17 eV at 300 K), we shall not consider it in the following.

Before discussing these data, a few comments should be made on the actual reliability of the application of photoacoustic spectroscopy to the investigation of the optical properties of USPSL. In Fig. 3 we compare the PAS spectrum with the low-temperature photoluminescence and photoluminescence excitation spectra (PLE) obtained

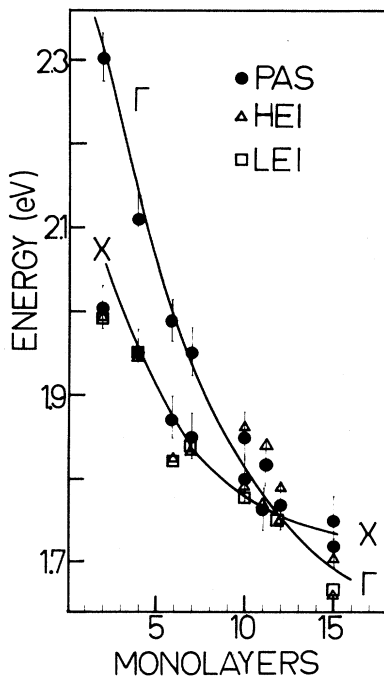


FIG. 2. Theoretical calculation of the energy of the quantized subbands in the  $\Gamma$  point of the GaAs and in the  $X$  point of the AlAs as a function of monolayers constituting the well and barrier in the GaAs/AlAs USPSL (solid lines) at 10 K ( $m=n$ ). The calculations are compared with the results of the PAS measurements (dots) and with the results of the LEI and the HEI photoluminescence measurements discussed in the text (squares and triangles, respectively). The PAS data have been scaled in energy by the temperature shift occurring between 300 and 10 K to be compared. The error bars represent the uncertainty in the PAS measurements.

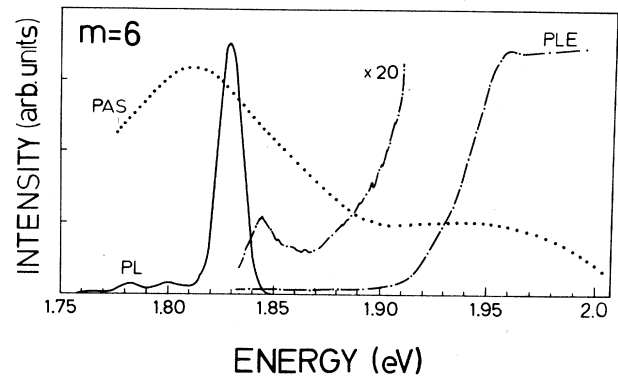


FIG. 3. Comparison between the PAS spectrum (dotted line) and the photoluminescence (solid line) and photoluminescence excitation (dot-dashed line) spectra for a  $(\text{GaAs})_6/(\text{AlAs})_6$  USPSL recorded at 10 K. The PAS spectrum has been scaled in energy by the temperature shift occurring between 10 and 300 K.

from the USPSL  $(\text{GaAs})_6/(\text{AlAs})_6$ . In agreement with the results of Refs. 2, 4, and 5, the PLE of this indirect USPSL exhibits a small peak localized around the energy of the type-II luminescence and a sharp onset corresponding to the increasing absorption at the  $\Gamma$  point. A satisfactory overall agreement in the energy positions of the  $X$ - and  $\Gamma$ -point transitions is found when comparing the PLE and the PAS spectra within the limited accuracy of the PAS technique of about 30 meV. Nevertheless, a few points related to the interpretation of the PAS spectra should be discussed. First, the photoacoustic-saturated regime is probably fully reached only in the spectral range of the  $\Gamma$ -point transitions (high-absorption coefficient) but not in the  $X$  range [having a smaller  $\beta(\lambda)$ ]. It is, therefore, expected that the PAS spectrum cannot give any quantitative information on the strength of the investigated absorption processes. Second, the fraction of the absorbed light converted into heat inside the crystal [the  $\alpha(\lambda)$  factor included in the proportionality factor in Eq. (2)] can be actually larger for the low radiative efficiency transitions, i.e., typically for the type-II transitions at the  $X$  point of the AlAs, thus affecting the relative intensity of the observed peaks in the PAS spectra. Nevertheless, although these limitations can reduce the actual amount of information provided by the PAS technique, it still has some advantages that should be mentioned. First of all, it is particularly suitable for the direct investigation of the band-structure properties of the superlattices at room temperature when the luminescence efficiency is considerably reduced (especially the type-II luminescence) and the PLE technique cannot be applied. In addition, the PAS spectroscopy allows a determination of the energies of the fundamental transitions in crystals with an accuracy that, although not comparable to the accuracy achieved in PLE or PL measurements, is sufficient to investigate the electronic transitions occurring between closely spaced critical points.

In conclusion the PAS technique gives information on the band-structure properties of the USPSL and can be

considered a complementary tool for the optical investigation of these complex heterostructures.

### B. Luminescence spectroscopy

The data of Fig. 2 indicate that the transition from a type-I to type-II superlattice should occur around  $m=n=12$  in the GaAs/AlAs system. To our knowledge no direct observation of this transition in luminescence has yet been reported. Previous experiments<sup>1-5</sup> have shown that in type-I superlattices the main luminescence band, originating from the direct recombination of electrons confined in the  $\Gamma$  point of the GaAs well, occurs at an energy nearly coincident with the fundamental absorption edge observed in the PLE spectra. Conversely, in type-II superlattices the main luminescence emission, which is related to the radiative recombination of electrons confined in the low-lying  $X$  point of the AlAs, occurs at an energy lower than the fundamental absorption edge in the PLE spectra. The reduced overlap of the electron and hole wave functions localized in different layers of the heterostructure makes this transition less probable than the direct one, thus causing the attenuation of the luminescence intensity in the type-II superlattices.

The results of the photoacoustic measurements discussed in Sec. III A allow us to directly compare the photoluminescence spectra with the expected energy-band scheme in USPSL with different configurations. In Fig. 4(a) we show the low-intensity photoluminescence of a typical type-II  $(\text{GaAs})_2/(\text{AlAs})_2$  USPSL. It can be observed that this emission band lies around the energy corresponding to the spatially indirect  $X$ -point transition already observed in the PAS spectrum. The emission line shape is slightly broadened in the low-energy side due to the presence of some impurity or defect-related emission which has been observed to disappear by increasing the temperature. In Fig. 4(b) we also show the high-intensity luminescence of the  $m=n=2$  USPSL obtained with pulsed excitation. The application of intense excitation (below the stimulation threshold) provides important information on the recombination mechanisms of the indirect-gap materials,<sup>8</sup> since it allows the observation of emission processes from different critical points, provided they are not too far in energy. This phenomenon is due to the simultaneous population of the two gaps resulting from the band filling induced by the stationary optical pumping. In our case this can occur once the fast transfer of electrons from the GaAs  $\Gamma$  point to the AlAs  $X$  point has taken place.<sup>9</sup> Since the observed energy separation between the GaAs  $\Gamma$  point and the AlAs  $X$  point in the  $m=n=2$  USPSL is of the order of 300 meV (see Figs. 1 and 2), this configuration behaves essentially like a type-II superlattice. No direct observation of the  $\Gamma$ -point luminescence is possible even under pulsed HEI conditions.

It is worth noting that the exciting power density employed in the measurements (i.e.,  $I_0=300 \text{ kW cm}^{-2}$ ) corresponds to an estimated photogenerated electron-hole density of the order  $10^{12} \text{ cm}^{-2}$  (calculated by using the relaxation time recently measured by Göbel *et al.* in

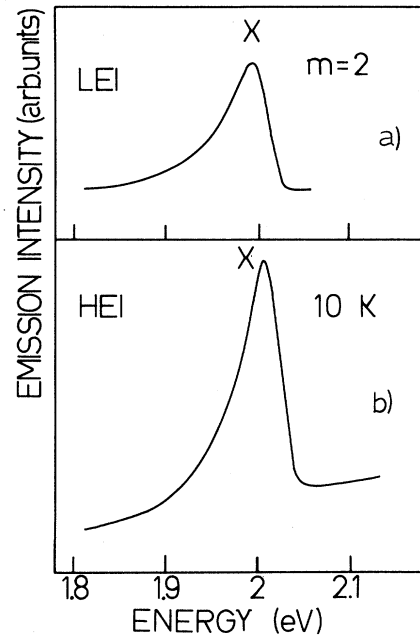


FIG. 4. (a) Low-excitation intensity (LEI) continuous-wave photoluminescence spectrum and (b) pulsed high-excitation intensity (HEI) emission spectrum obtained from the  $(\text{GaAs})_2/(\text{AlAs})_2$  USPSL at 10 K.

these USPSL<sup>9</sup>. The estimated band filling in the energy space is of the order of 50 meV under these conditions. It is, therefore, evident that direct observation of the  $\Gamma$ -point luminescence is possible only when the energy separation between the direct and the indirect subbands in the superlattice is of the order of 50 meV, i.e., approaching the type-I–type-II crossover. This is clearly shown in the data of Fig. 5 where the LEI and the HEI luminescence spectra of a  $(\text{GaAs})_{10}/(\text{AlAs})_{10}$  USPSL are compared. In agreement with previous observations,<sup>1,5</sup> the low-intensity photoluminescence spectrum [Fig. 5(a)] shows the spatially indirect radiative recombination associated with the lowest-energy subband in the  $X$  point of the AlAs barrier. The low-energy shoulders are probably due to phonon-assisted transitions and to impurity-related complexes. The energy position of this luminescence band is consistent with the  $X$  maximum position observed in the PAS spectrum and with the calculated transition energy (once the temperature shift is accounted for).

Conversely, a completely different behavior is observed in the HEI spectra. In Fig. 5(b) several emission spectra recorded at different excitation power densities are shown. The most important feature is that at the lowest intensity the HEI spectrum coincides with the cw spectrum, and only type-II recombination is observed. When increasing the photogenerated  $e-h$  density, the higher-energy subband in the GaAs well becomes populated, and a strong direct emission is observed in the spectra. This  $\Gamma$  emission appears at an energy position coincident with the observed  $\Gamma$  level of the GaAs quantum well in the

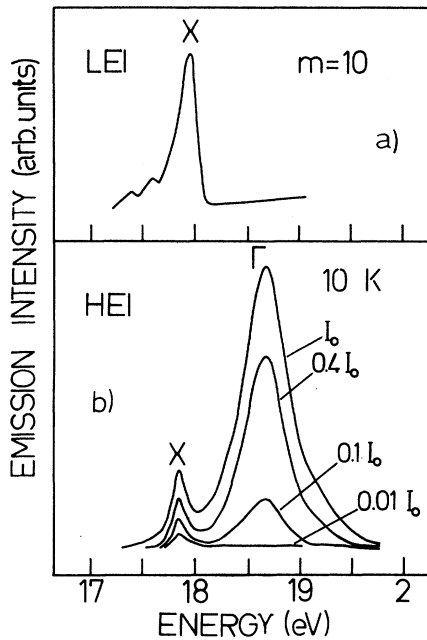


FIG. 5. Emission spectra as in Fig. 4 for the  $(\text{GaAs})_{10}/(\text{AlAs})_{10}$  USPSL. The pulsed excitation spectra have been recorded at different intensities.

PAS spectrum. The direct emission grows superlinearly up to the highest excitation levels, while the indirect  $X$  luminescence saturates as expected from the different relaxation times of the two recombination processes.<sup>9</sup> In addition the  $\Gamma$  emission is much more intense than the  $X$  one, as expected for the direct transition involving  $\Gamma$  electrons and holes in the GaAs well. These results suggest that the  $(\text{GaAs})_{10}/(\text{AlAs})_{10}$  USPSL is close to the critical layer thickness for the transition from a type-I to type-II superlattice. This assumption is confirmed by the results of Fig. 6 where we show the LEI and HEI luminescence spectra recorded in the USPSL with  $m = n = 15$ . In this case the most important feature is that the cw spectrum and the main luminescence band in the HEI spectra coincide in energy and are consistent with the theoretical position of the direct  $\Gamma$  transition in the GaAs well and also with the results of the PAS measurements. The coincidence of the two spectra confirms the type-I behavior of this superlattice. It should be mentioned that according to the direct character of the recombination, in this superlattice we observe a considerable increase of the LEI photoluminescence efficiency, which becomes now comparable to that of standard multi-quantum-well heterostructures usually investigated. By increasing the excitation intensity we observe a shoulder appearing on the high-energy side of the pulsed luminescence spectra. This is clearly related to the emission resulting from the indirect  $X$  point in the AlAs (actually lying at a slightly higher energy than the GaAs  $\Gamma$  point) and represents the weak contribution of a type-II transition caused by the band filling in the higher-energy  $X$  subband.

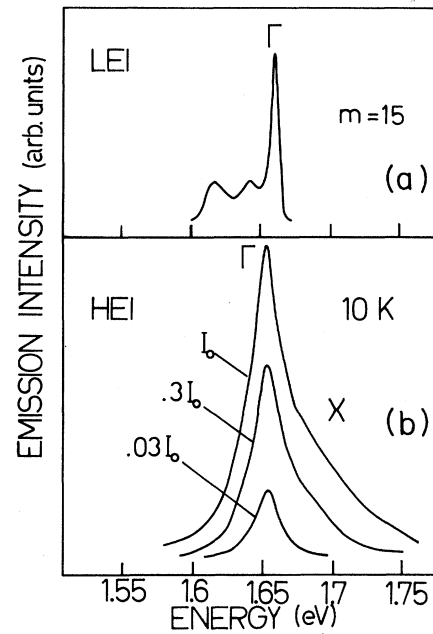


FIG. 6. Emission spectra as in Fig. 5 for the  $(\text{GaAs})_{15}/(\text{AlAs})_{15}$  USPSL.

The reported results clearly show the competition between the type-I and type-II recombinations in these USPSL. The direct observation of both the direct and the indirect emission provided by the high-intensity excitation well accounts for the band-structure features observed in the PAS spectra and for the low-intensity photoluminescence characteristics. It is worth noting that the use of these spectroscopic methods allows the accurate determination of the type-I-type-II crossover. This is exemplified by the results of Fig. 7, where the HEI luminescence spectra of USPSL near the direct-indirect transition (i.e.,  $10 < m, n < 15$ ) are shown. The spectra clearly reveal the observed transition from the type-II superlattice ( $m = n = 10$ ), characterized by the low-energy  $X$  emission to the type-I superlattice ( $m = n = 15$ ) already discussed. The crossover can be identified around  $m = n = 12$ , where the two emission channels almost overlap. These results are in agreement with the PAS spectra of the  $(\text{GaAs})_{12}/(\text{AlAs})_{12}$  USPSL which shows a unique maximum in which the  $\Gamma$  and the  $X$  features seem to be merged.

The photoluminescence data collected from all the investigated samples are displayed in Fig. 2 together with the PAS data for a better comparison. It is evident that all the data are in good agreement within the experimental accuracy and the precision of the calculation.

Finally, we want to briefly discuss the temperature dependence of the type-I and type-II emissions in the GaAs/AlAs USPSL. In Fig. 8(a) we show the temperature evolution of the  $X$  and the  $\Gamma$  luminescence in the  $(\text{GaAs})_{10}/(\text{AlAs})_{10}$  superlattice. As expected from the different temperature shifts of the  $\Gamma$  and  $X$  points of

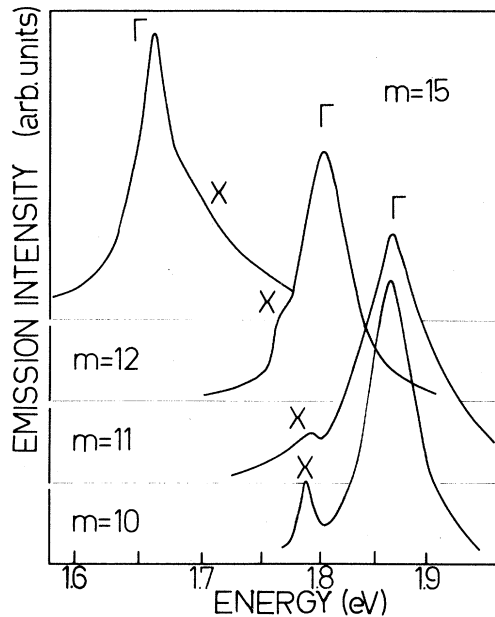


FIG. 7. Transition from a type-I to a type-II superlattice indicated in the HEI emission spectra for USPSSL with  $10 < m = n < 15$  at 10 K.

GaAs and AlAs, respectively, the two bands approach in energy by increasing the temperature. The integrated emission intensities of the two luminescence lines are depicted in Fig. 8(b). The most important feature is that the type-II recombination is strongly quenched by the temperature increase, disappearing above 40 K. The quenching of the  $X$  band coincides with the enhancement of the type-I luminescence which grows up to about 180 K. For further increasing temperatures the  $\Gamma$  luminescence weakens more and more until it reduces by an order of magnitude at room temperature. It is worth noting that this effect cannot be ascribed to a temperature-induced type-I–type-II transition since in the LEI luminescence spectra the type-II emission is dominant up to 80 K [see Fig. 7(b)] and no  $\Gamma$  emission is observed even at higher temperatures. The thermal transfer of  $X$  electrons to the quasiresonant subband, induced by the increase of the statistical population or by the  $\Gamma$ - $X$  scattering in the photogenerated electron-hole plasma, can be tentatively invoked to give a qualitative explanation of our observation. The depletion of the  $X$  point and the consequent population increase in the direct quasiresonant  $\Gamma$  state can also explain the enhancement of the type-I luminescence occurring at the same temperature at which the  $X$  band disappears. Although the study of these kinds of processes is beyond the aim of this paper, we believe that other effects, like the change in the overlap of the wave function of electrons and holes confined in different slabs of the superlattice, or the thermal activation of nonradiative centers at the interfaces,<sup>10</sup> should also be taken into account to give a rigorous explanation of the observed temperature dependence of the luminescence.

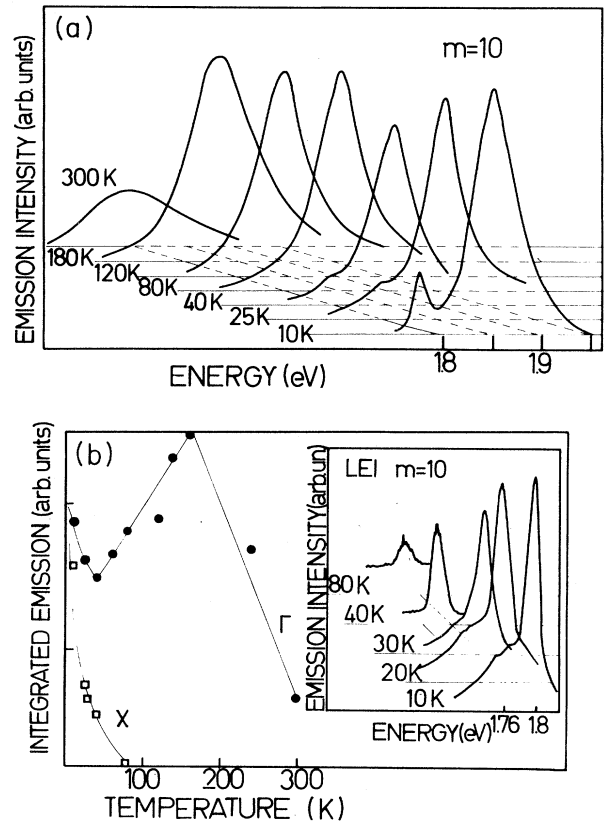


FIG. 8. (a) HEI emission spectra of  $(GaAs)_{10}/(AlAs)_{10}$  USPSSL recorded at different temperatures. (b) Temperature dependence of the integrated emission intensity of the  $\Gamma$  and  $X$  bands. The LEI of the same USPSSL at different temperatures is shown in the inset.

#### IV. CONCLUSIONS

The type-I–type-II transition occurring in ultra-short-period GaAs/AlAs superlattices at critical layer thicknesses has been investigated by means of different spectroscopic techniques. Information on the band structure of these superlattices has been obtained by means of photoacoustic saturation spectroscopy. We have found that the crossover between direct and indirect optical transitions in the GaAs/AlAs USPSSL occurs when the wells and the barriers are each composed of 12 monolayers. The results of the photoacoustic spectroscopy are closely related to the results of photoluminescence measurements. Emission spectroscopy under intense pulsed excitation allowed the direct observation of the radiative recombinations from both the electrons confined in the GaAs  $\Gamma$  point and in the AlAs  $X$  point when the constituent layer thickness was around the critical value of  $m = n = 12$ . The optically determined direct and indirect transition features are in good agreement with the results of PAS measurements and with theoretical calculations. Finally, the temperature dependence of the type-I and type-II emissions exhibits a nonmonotonic behavior which has been tentatively ascribed to the thermal transfer of electrons between the critical points in the different confinement regions.

- \*Present address: Max-Planck-Institut für Festkörperforschung, Heisenbergstrasse 1, Postfach 80 06 65, D-7000 Stuttgart 80, Federal Republic of Germany.
- <sup>1</sup>For a recent review see B. A. Wilson, *IEEE J. Quantum Electron.* **QE24**, 1763 (1988).
- <sup>2</sup>G. Danan, B. Etienne, F. Mollot, R. Planel, A. M. Jean-Louis, F. Alexandre, B. Jusserand, G. Le. Roux, J. Y. Marzin, H. Savary, and B. Sermage, *Phys. Rev. B* **35**, 6207 (1987).
- <sup>3</sup>E. Finkman, M. D. Sturge, M. H. Meynadier, R. E. Nahory, M. C. Tamargo, D. M. Hwang, and C. C. Chang, *J. Lumin.* **39**, 57 (1987).
- <sup>4</sup>D. S. Jiang, K. Kelting, T. Isu, H. J. Queisser, and K. Ploog, *J. Appl. Phys.* **63**, 845 (1988).
- <sup>5</sup>K. J. Moore, G. Duggan, P. Dawson, and C. T. Foxon, *Phys. Rev. B* **38**, 5535 (1988).
- <sup>6</sup>Huang-Sik Cho and P. R. Prucnal, *Phys. Rev. B* **36**, 3237 (1987).
- <sup>7</sup>L. Baldassarre and A. Cingolani, *Phys. Scr.* **37**, 385 (1988).
- <sup>8</sup>R. Cingolani, M. Ferrara, and M. Lugarà, *Phys. Rev. B* **36**, 9589 (1987).
- <sup>9</sup>E. O. Göbel, R. Fischer, G. Peter, W. W. Rühle, J. Nagle, and K. Ploog, in *Optical Switching in Low Dimensional Systems*, edited by H. Haug and L. Banyai (Plenum, New York, 1988).
- <sup>10</sup>S. Tarucha and K. Ploog, *Phys. Rev. B* **38**, 4198 (1988).